Towards a New Modality-Independent Interface for a Robotic Wheelchair

Teodiano Freire Bastos-Filho, Fernando Auat Cheein, *Member, IEEE*, Sandra Mara Torres Müller, Wanderley Cardoso Celeste, Celso de la Cruz, Daniel Cruz Cavalieri, Mário Sarcinelli-Filho, Paulo Faria Santos Amaral, Elisa Perez, Carlos Miguel Soria, and Ricardo Carelli, *Senior Member, IEEE*

***Abstract*—This work presents the development of a robotic wheelchair that can be commanded by users in a supervised way or by a fully automatic unsupervised navigation system. It provides flexibility to choose different modalities to command the wheelchair, in addition to be suitable for people with different levels of disabilities. Users can command the wheelchair based on their eye blinks, eye movements, head movements, by sip-and-puff and through brain signals. The wheelchair can also operate like an auto-guided vehicle, following metallic tapes, or in an autonomous way. The system is provided with an easy to use and flexible graphical user interface onboard a personal digital assistant, which is used to allow users to choose commands to be sent to the robotic wheelchair. Several experiments were carried out with people with disabilities, and the results validate the developed system as an assistive tool for people with distinct levels of disability.**

***Index Terms*—Assistive devices, assistive technology, biomedical transducers, service robots, wheelchairs.**

I. Introduction

ONE of the difficulties found by people with disabilities is related to their mobility. Common wheelchairs require from the user their intact manipulation ability, to use a joystick to navigate the vehicle. However, many people with disabilities do not have this manipulation ability or similar mechanical device, thus being unable to use this kind of wheelchair [1]. As an example, users suffering of amyotrophic lateral sclerosis (ALS) have quite low mobility, and can loose their communication capabilities, becoming locked in their own body, with low quality of life, which generates frustration, anxiety, and depression [2].

Robotic systems can improve the personal autonomy of people with disabilities through the development of some devices that allow them to move and to communicate. A robotic wheelchair can be used for mobility for people who are unable to manipulate joysticks, providing to them some level of mobility and freedom.

Smart wheelchairs are target of studies since beginning of 1980s, with several developments in different countries, with wheelchair being commanded by eye blinks, eye movements, facial/head gestures, blowing and suck (also named "sip and puff switch"), and brain waves, and providing navigation assistance to users in different ways, such as assuring collision-free travel, aiding the performance in accomplishing specific tasks (e.g., passing through doorways), and autonomously transporting the user between predefined locations, such as follows [3]–[11]: the wheelchair of the Smart Alec Project at Stanford University (1980) used ultrasonic sensors to detect the user's position. The wheelchair by Madarasz (1986) of Arizona State University was also equipped with ultrasonic sensors and was able to navigate in corridors.

The NavChair of University of Michigan (1993) was built to avoid obstacles, follow walls, and travel safely in cluttered environments using ultrasound sensors. The wheelchairs named Tin Man I and Tin Man II, of KISS Institute for Practical Robotics, had three operation modes: human guided with obstacle avoidance, move forward along a given heading, and move to a desired position (Tin Man I), while Tin Man II had the capabilities of wall following, doorway passing, and docking to objects such as tables. The wheelchair of University of Pennsylvania (1994) was equipped with two legs, in addition to the four regular wheels; the legs enabled the wheelchair to climb stairs and move through rough terrain.

The Wheelesley (1995) of MIT was a wheelchair equipped with infrared proximity sensors and ultrasonic range sensors, and used switches on a panel onboard to choose among different high level movement commands such as forward, left, right, stop, or drive backwards, and also be maneuvered with an eye tracking interface. The Smart Wheelchair (1995) of University of Edinburgh had bump sensors to sense obstacles and had a line following algorithm for driving through doors and between rooms. The Orpheus (1996) of University of Athens was a wheelchair equipped with 15 ultrasonic sensors for localization and obstacle avoidance, and had four basic actions: move straight, turn left, turn right, and reverse. The wheelchair developed in TAO Project (1996) of Applied AI Systems Inc., had functions for collision avoidance, driving in narrow corridors and driving through narrow doorways, using two color cameras to identify colored landmarks. The interfaces onboard were a microphone, a keypad, and a joystick. With the voice the user

Manuscript received November 19, 2012; revised April 02, 2013; accepted May 19, 2013. Date of publication June 04, 2013; date of current version April 28, 2014. This work was supported in part by FAPES/Brazil (Process 39385183/2007), in part by FACITEC/Brazil (Process 061/2007), and in part by CAPES/Brazil-SPU/Argentina (Process 044/2010 CAPG-BA).

T. F. Bastos-Filho, S. M. T. Müller, W. C. Celeste, C. de la Cruz, D. C. Cavalieri, M. Sarcinelli-Filho, and P. F. S. Amaral are with the Department of Electrical Engineering, Federal University of Espírito Santo (UFES), 29073-910 Vitória, Brazil (e-mail: teodiano@ele.ufes.br; mario.sarcinelli@ufes.br).

F. A. Cheein is with the Department of Electronics Engineering, Universidad Tecnica Federico Santa Maria, 1680 Valparaiso, Chile (e-mail: fernando.auat@usm.cl).

E. Perez, C. M. Soria, and R. Carelli are with Instituto de Automática, Universidad Nacional de San Juan (UNSJ), J5400 San Juan, Argentina (e-mail: csoria@ianut.unsj.edu.ar).

Color versions of one or more of the figures in this paper are available online at http://ieeexplore.ieee.org.

Digital Object Identifier 10.1109/TNSRE.2013.2265237

was able to activate functions such as stop, turn left, turn right, and drive. The Rhombus (Reconfigurable Holonomic Omnidirectional Mobile Bed with Unified Seating) of MIT (1997) was a wheelchair with omni-directional drive, and could be reconfigured into a bed. The RobChair (1998) of University of Coimbra was a wheelchair equipped with five wheels, and could be operated by voice, keyboard, and/or by an analog joystick. It had 12 infrared sensors, four ultrasonic sensors, and one tactile bumper.

The INRO (Intelligenter Rollstuhl) of University of Applied Sciences Ravensburg–Weingarten (1998) was a wheelchair whose main objective was to support users with disabilities in navigation and for obstacle detection. The Intelligent Wheelchair System of Osaka University (1998), had two cameras: one facing towards the user and the other facing forward. User provided input to the system with head gestures, interpreted by the inward-facing camera. The Smart Wheelchair of University of Plymouth (1998) used a controller based on neural networks to trace predefined paths autonomously within an art gallery. The Luoson III of National Chung Cheng University (1999) was a wheelchair equipped with a force reflection joystick, video camera, ultrasonic sensors, digital compass, gyroscope, and microphone. It had three operating modes: direct control, assistive control, and autonomous control.

The OMNI (Office wheelchair with high Maneuverability and Navigational Intelligence) of University of Hagen (1999) had omnidirectional steering and was equipped with ultrasonic sensors and an infrared detector for real-time obstacle avoidance and back tracing. The Tetranuta (1999) of University of Seville was a wheelchair that provided autonomous navigation by landmarks painted on the floor and landmarks in the form of radio beacons. The Hephaestus of TRACLabs (1999) was a wheelchair with 16 ultrasonic sensors, configured to detect obstacles. The SIAMO project at University of Alcala (1999) was used as a test bed for various input methods (voice, face/head gestures, EOG) for the wheelchair. The voice-cum-auto steer wheelchair of CEERI (India, 1999) could autonomously travel to a given destination based on internal map or by following tape paths on floor.

The FRIEND (Functional Robot arm with user-friendly Interface for Disabled people) of University of Bremen (2001) had two parts: a wheelchair, and a six degree-of-freedom robot arm. Both devices were controlled by a speech recognition system. The wheelchair used stereo vision and a camera mounted in the gripper for obstacle detection. The Rolland I (2001) of University of Bremen was a wheelchair equipped with 27 ultrasonic sensors and a laser range finder for navigation. The MAid (Mobility Aid for Elderly and Disabled People) of University of Ulm (2001) was a wheelchair equipped with ultrasonic sensors, two infrared scanners and a laser range finder. The VAHM (acronym French for *autoVehicule Autonome pour Handicape Moteurnomous*) of University of Metz (1993, 2001) was a wheelchair with two versions. First, the wheelchair was placed on the top of a mobile robot base, and could follow walls and avoid obstacles. In a second version, a powered wheelchair was used, and a grid based method was used for navigation.

The Argyro's Wheelchair of Institute of Computer Science (Greece, 2002) could avoid obstacles and follow a person. It was equipped with ultrasonic sensors and an omnidirectional camera. The WAD Project of Centre National de la Recherche Scientifique (CNRS) (2002) was a wheelchair that could avoid obstacles through infrared sensors. The SmartChair of University of Pennsylvania (2002) was equipped with wheel encoders, an omnidirectional camera, infrared sensors, a laser range finder, and an interaction camera, and had six behaviors (control modes): hallway navigation, three-point turn (reversing and turning), obstacle avoidance, navigate through a doorway, turn while avoiding obstacle, and go to a specific goal. The SIRIUS of University of Seville (2002) was a wheelchair that could be teleoperated, run autonomously, or be manually controlled.

The Collaborative Wheelchair Assistant of National University (Singapore, 2002) allowed users to travel according to software-defined paths. The HaWCos of University of Siegen (2002) was a wheelchair that used muscle contractions as input signals. The DREAM-3 of Tottori University (2004) was a wheelchair that had five action patterns: follow the left wall, follow the right wall, turn left, turn right, and drive forward. The SWCS (Smart Wheelchair Component System) of University of Pittsburgh (2004) navigated using information from ultrasonic sensors, infrared, and bump sensors. The Victoria, of Aachen University (2004), was a wheelchair equipped with two computers and a touch screen, cameras, and a manipulator. The user could select, through the touch screen, an object that the manipulator should grasp. A grasped object could be placed on the wheelchair table, kept in the gripper, or held near the face of the user. The SPAM (Smart Power Assistance Module) of University of Pittsburgh (2005) was a wheelchair that used information from different types of sensors (ultrasonic and infrared) for navigation. Torque sensors were used to measure the manual forces applied to the wheels such that the system could add additional torque to assist the user and reduce the risk of fatigue.

The Rolland III of University of Bremen (2005) was a wheelchair equipped with two laser range finders (one locking forward and one backwards), encoders and an omnidirectional camera (used to find features in the environment). The TAO Aicle of AIST (National Institute of Advanced Industrial Science and Technology of Japan, 2006) was a wheelchair that used information from laser range finder, GPS, compass, and radio-frequency identification (RFID) technology for navigation. The Walking Wheelchair of University of Castilla-La Mancha (2006) was equipped with four wheels and four legs. The legs made possible the wheelchair to climb stairs. The WASTON Project of NAIST (Japan, 2001) was a wheelchair with machine vision to interpret user's gaze and controlling the wheelchair.

The Smart Wheelchair developed in the University of Hong Kong (2002), used neural networks to map sensor readings to control actions to play back taught routes. The HURI Project of Yonsei University (2002–2003) was a wheelchair with machine vision to identify facial gestures of the user. The WAD Project of Bochum University (2002) was a wheelchair that either navigated autonomously to a desired position or provided obstacle avoidance while the user navigates. The Niigata University (2004) developed a wheelchair that used EOG signals to command a cursor to displace in four directions (up, down, left, and right) while one blink of the eye selected the icon. The

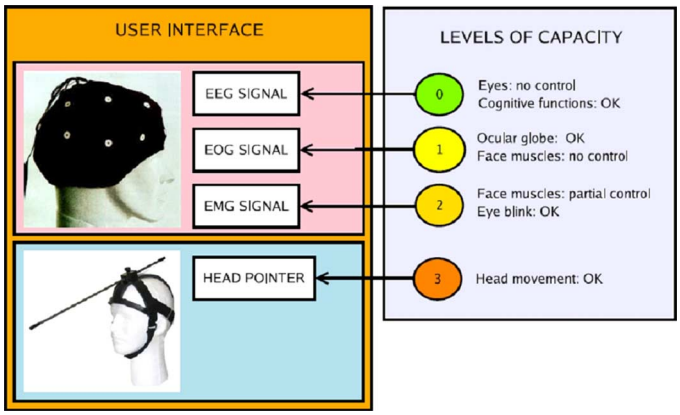

Fig. 1. Different modalities to operate the robotic wheelchair, and the corresponding levels of capacity. Adapted from [12].

University of Electro-communication (Japan) and University of Boston (USA), in 2004, developed a wheelchair that could be commanded by brain waves, using 13 EEG electrodes. The University of Zaragoza (2009) developed a wheelchair commanded by voice, blowing, and brain waves.

The robotic wheelchair of Ecole Polytechnique Federale de Lausanne (EPFL, 2010) used camera, laser and ultrasonic sensors, plus a collaborative controller, to help users to drive safely the wheelchair commanding it through of eye movements. The ARTY (Assistive Robot Transport for Youngsters) of Imperial College London (2011) was a pediatric wheelchair equipped with ultrasonic and infrared sensors, which could be commanded by children through head movements (captured by a gyroscope on a hat). The IDIAP Research Institute (2011) developed a wheelchair that could be commanded by brain waves. The Pohang University of Science and Technology (2012) uses tongue movements to command a wheelchair, and the Federal University of Espírito Santo (UFES/Brazil, 2012) developed a robotic wheelchair with a unified platform. This wheelchair is equipped with sensors to detect and avoid obstacles, and is able to follow a predefined path or a path chosen by the user to get to a wished destination place. The commands for the wheelchair can come from the user, through eye blinks, eye movements, head movements, sip-and-puff, or brain signals.

Users with good head posture and control of head movements may use an Inertial Measurement Unit (IMU) attached to his/her head or a video camera installed onboard the wheelchair to capture their head movements. However, users without head movements, but with the ability of sip-and-puff—captured by a pressure sensor into a straw—or blink their eyes—captured by surface myoelectric signals (sEMG)—could use these modalities to operate the wheelchair.

On the other hand, people with ALS can be unable to blink their eyes but can use their eye movements to generate commands, using electro-oculography (EOG)—captured by surface myoelectric signals—or video-oculography (VOG) methods—through a video camera. Moreover, brain waves—obtained from electroencephalogram (EEG)—may also be used to operate the wheelchair through a brain–computer interface (BCI).

Fig. 1 presents the modalities that can be used by people with disabilities to operate the wheelchair here developed. For example, head mounted-IMU or camera based systems may be the preferred alternative for those with good control of the head, but for some users (e.g., with cerebral palsy) with no accurate motor control of the head, sip-and-puff, eye blinks or EOG/VOG can be preferred as control modalities. EEG is a suitable alternative left for some type of users, e.g., suffering from locked-in syndrome. Other modalities of using this wheelchair are as an auto-guided vehicle or as an autonomous vehicle. In addition the latter, this wheelchair has a communication system onboard which allows users to communicate with people around the wheelchair.

This work is aimed at reporting a new modality-independent interface designed to command the robotic wheelchair developed by the Federal University of Espirito Santo (Brazil). Briefly, the robotic wheelchair can be commanded either by eye-movements, eye-blinks, face and head movements, sip-and-puff, gravitational acceleration and superficial brain signals, with the aim of offering a solution to a wide range of disabilities. Additionally, the robotic wheelchair is able to perform under three behavioral modes: nonautonomous (the wheelchair is entirely controlled by the user), autonomous (a first approach uses a SLAM (simultaneous localization and mapping) algorithm for mapping and localizing the wheelchair within unvisited places; and a second approach uses metal tapes placed within a closed environment to guide the wheelchair for autonomous navigation within it); and a semi-autonomous behavior (the wheelchair command is shared by the user and an autonomous supervision system that prevents the wheelchair from collisions, dangerous or risky movements and allows for smooth motion while navigating the environment). The entire system is tested as a pilot study in a population of healthy and people with disabilities. However, this work reports in detail the evaluation of performance of seven volunteers with different disabilities. The questionnaire used to evaluate the performance of the interface and the wheelchair, as well as experimental and statistical results showing the pros and cons of each proposal, are also included herein.

This work is structured as follows. Section II introduces the robotic wheelchair developed by the Federal University of Espirito Santo (Brazil), which is referenced in the sequel. Section III presents the human–machine interface (HMI) developed and different modalities presented in this work. Section IV shows the navigation interface used by the modalities presented herein. Section V presents both statistic and metric results of the different modalities tested in a population of seven volunteers with different capabilities. Section VI highlights the discussions and conclusions of our work.

II. Robotic Wheelchair

The robotic wheelchair used in this work is shown in Fig. 2. Briefly, the robotic wheelchair consists of two differential motors (one per each traction wheel) and a main micro-controller (ArduPilot MEGA) as low level controller. Each traction wheel has its own optical encoder, whose measurements are sent to the micro-controller. The high level control and the interfaces developed in this work, are connected to a laptop computer, which processes all the incoming data. Via USB-port, the laptop computer sends the motion commands to the wheelchair and reads

Fig. 2. Robotic wheelchair with laser range sensor mounted on its footrest.

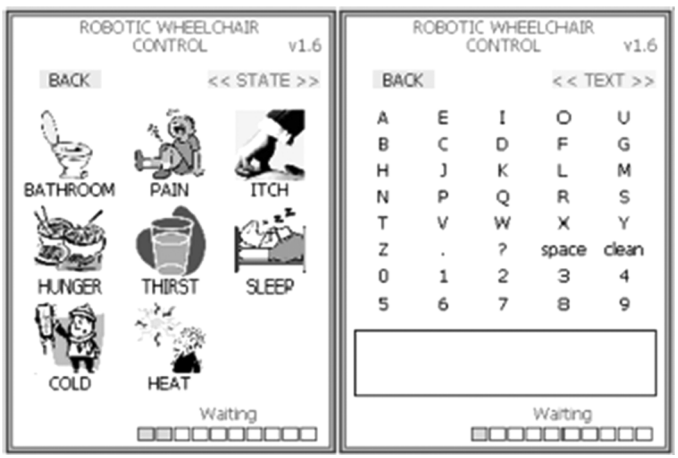

Fig. 3. Different options of communication (symbols representing needs or feelings, or characters).

the encoders measurements. Additionally, the computer is able to access the accelerometers readings of the ArduPilot. A range laser SICK is incorporated in the footrest of the wheelchair. The range laser is used for mapping and autonomous navigation, as mentioned in Section III-G. As can be seen, the laser sensor does not increase the mobility restrictions of the wheelchair. Additionally, a path planning algorithm presented in Section III-G2 guarantees that the wheelchair will reach the desired destination and orientation within the environment [13]. Further information regarding the wheelchair sensing and programming can be found in [13], [14].

In addition, the robotic wheelchair is equipped with a communication system onboard: a PDA. Such a PDA provides with a graphical user interface (GUI) with icons for communication symbols (characters and icons expressing needs or feelings), as illustrated in Fig. 3. They are organized in a hierarchical way, and scanned serially although, they can also be manually accessed. Once a valid command is identified, a suitable prerecorded acoustic emission is transmitted to the speakers onboard the wheelchair, according to the symbol, word, or sentence selected, allowing users to communicate with people around. The user of the wheelchair, through the PDA, is also able to interchange among the different modalities of control presented in

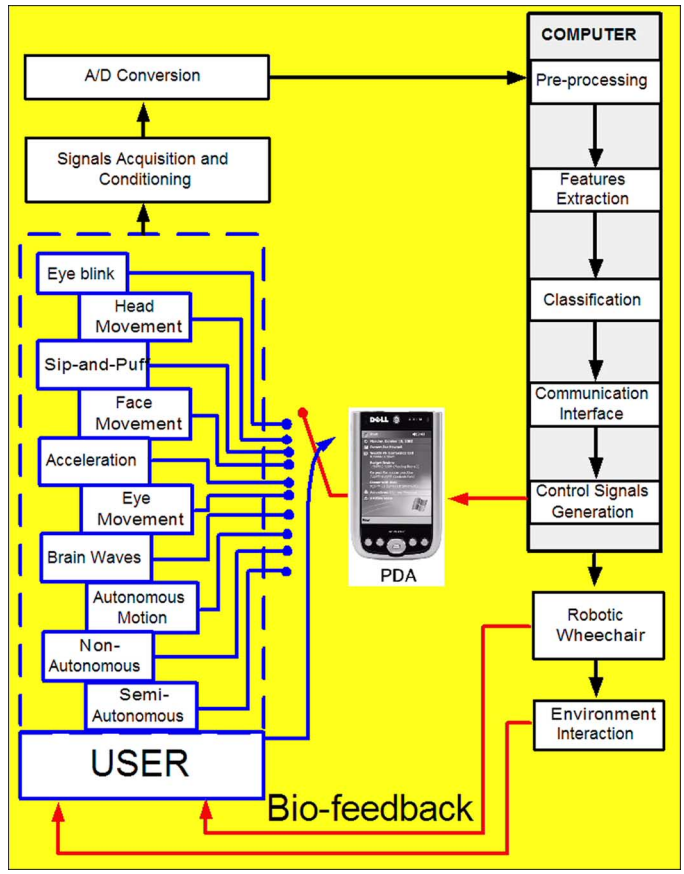

Fig. 4. General architecture of the HMI developed.

this work: eye blinks, head movements, face movement, sip-and-puff, gravitational acceleration, eye movements, semi-autonomous navigation, and autonomous navigation.

Fig. 4 illustrates how this whole system can be interchangeable among the paradigms used to navigate the wheelchair. The framework of the developed HMI can be divided into three main parts.

1) The signal acquisition system, which represents the acquisition, conditioning, preprocessing of the signals of sEMG (surface electromyogram), EEG (electro encephalogram), sip-and-puff, gravitational acceleration, and video.
2) The computational system, represented in these figures by the block called COMPUTER, which is responsible for processing and classifying the information coming from the conditioned acquired signal. This processing unit is related to the inherent processing unit of the PDA or even to a more sophisticated computational unit, such as a low-power computer (mini-ITX).
3) Output devices, which are related to command the wheelchair, but also present a graphical interface aiming at stimulating the users and informing them about the chosen command.

III. Human–Machine Interface

Fig. 4 shows the general structure of the HMI developed in this work. This interface consists of an acquisition system that includes amplification, filtering, digitization, recording, and

processing of different kinds of signals provided by the wheelchair user. The signals are recorded and classified in real-time, sending the identified class to a PDA. This PDA is responsible to generate commands of movement to a computer onboard the wheelchair. Once a valid command is identified, a movement command is sent to the actuators of the wheelchair.

As stated in Section II, the user is able to select the modality of control of the robotic wheelchair. There are six human-based interfaces for controlling the vehicle (by head, face, or eye movements, brain waves, blinks, gravitational acceleration, and sip-and-puff, as shown in Fig. 4), plus three navigation modes (autonomous, semi-autonomous, and nonautonomous). It is worth mentioning that the six human-based interfaces imply that the wheelchair will be commanded in an nonautonomous or semi-autonomous way only. The user of the wheelchair selects which interface or navigation mode will use. Such selection is made by the assistance of another person due to the fact that, as stated in Section II, the PDA can be manually handled or by using the current interface mode (e.g., if the interface was previously selected to perform using eye blinks, then the following interface or navigation mode can be selected by eye blinking).

Despite the selected interface modality, the biological signal is processed and converted in commands imparted to the PDA or to the wheelchair's motion. As the vehicles navigates within the environment, the loop of the architecture shown in Fig. 4 is closed by means of the *bio-feedback*: the user receives the information of the motion and the environment and corrects the commands generation by means of her/his own learning [15]. Following, each stage shown in Fig. 4 will be explained in detail.

A. Acquisition and Processing System

The system here reported is a noninvasive one and it is described as follows.

1) It determines eye blinks based on sEMG. This method requires the placement of surface electrodes on the temporal muscles around the eyes.
2) The eye movements are determined based on video data acquired through a small video camera attached to a pair of glasses (videooculography).
3) The head movements are captured using an inertial module unit (IMU) attached to a cap or a video camera installed in front of the wheelchair user.
4) The sip-and-puff is captured by a pressure sensor installed into a straw.
5) The EEG waves are acquired using a commercial EEG acquisition equipment.
6) The face movements are acquired using an onboard vision system.

B. Commanding the Robotic Wheelchair by Eye Blinks

Two channels of sEMG are used to command the robotic wheelchair using eye blinks. These sEMG signals are captured using two electrodes located on temporal muscles, as shown in Fig. 5. One channel is used for right eye muscle and the other for left eye muscle.

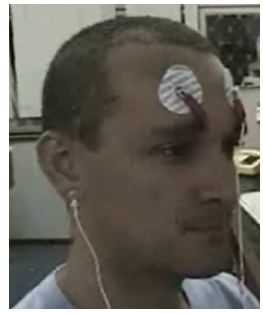

Fig. 5. Electrodes connection for the eye blinks interface modality.

Fig. 6. Robotic wheelchair commanded by eye blinks.

A simple threshold-based algorithm is used to detect the eye blink signals. The threshold is determined from the sample data, and corresponds to the value of 35% of the maximum peak of the sEMG signal, to avoid false detection.

The next step in confirming the valid eye-blink signal is based on its time duration. The algorithm developed is based on the angular variation of each sample. The tangent to the left and to the right of the signal peak derivative is computed. Case the tangent value is smaller than a threshold (0.0025 was empirically used), the correspondent time instant is considered the start or the end of the valid signal.

Once eye-blink signals are correctly detected, an artificial neural network (ANN) is used to recognize the eye blinks. As first step, data is down-sampled to 20 samples/s. These are then normalized to improve the speed of convergence of the ANN.

In this work, 252 test signals were obtained (84 eye blinks of the left eye, 84 eye blinks of the right eye, and 84 random noises). Several supervised ANN algorithms were evaluated, and a resilient backpropagation algorithm, with four neurons in the hidden layer and three neurons in the output layer, was used. With this algorithm, the successful rate in recognizing eye signals was 99.6%. Fig. 6 shows the robotic wheelchair commanded by eye blinks.

Despite the encouraging results obtained with this modality, one of its main drawbacks is that it is not suitable for users presenting muscle spasms or loss of muscle activity. Thus, next subsection presents another way to command the wheelchair, through head movements.

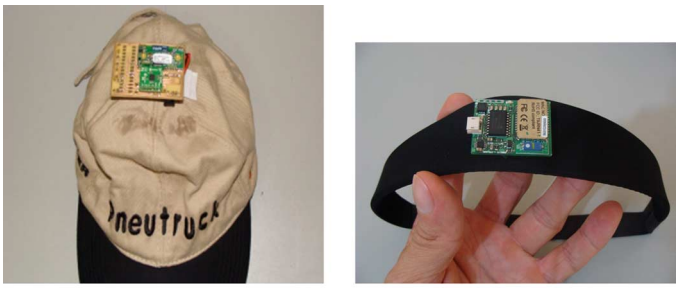

(a) (b)

Fig. 7. Inclination sensor based on IMU attached to different devices.

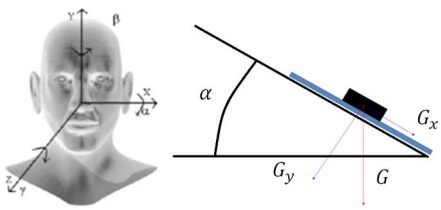

Fig. 8. Obtaining the inclination angle α.

Fig. 9. Robotic wheelchair commanded by a quadriplegic woman and a kid with Duchene dystrophy through their head movements (captured by IMU).

C. Robotic Wheelchair Commanded by Head or Face Movements

Two approaches have been provided for enabling the use of head movement to command the wheelchair. One approach uses an IMU attached to a cap (or other device attached to the head), mentioned as *gravitational acceleration* system in Section III. The second approach is a video-based system that uses an onboard video camera mounted in front of the wheelchair, focusing on the user's face.

1) Head Movements Modality: A two axis IMU is used to provide a voltage proportional to the head inclination. This signal is processed by a micro-controller which uses Bluetooth to communicate with the computer onboard the wheelchair [16]. Fig. 7 shows the sensor attached to a cap and the circuit developed to measure head movements. Moving the head forward, to the right or to the left implies to move the robotic wheelchair forward, to the right or to the left, respectively. Moving the head to the rear causes the stop of the wheelchair.

The principle for determining the head inclination angles is based on the associated gravitational accelerations. Two independent angles should be determined to obtain the head movement: α and γ angles. α is the forward inclination, which is codified to linear velocity of the robotic wheelchair while γ is the side inclination, which is codified to angular velocity. Fig. 8 shows how to obtain α (γ can be obtained exchanging Gy by Gz, the accelerations in the x and y-coordinates, respectively) as shown in

$$\alpha = \cos^{-1}\left(\frac{Gy}{G}\right). \tag{1}$$

Additionally, Fig. 9 shows the robotic wheelchair commanded by people with disabilities through their head movements. The statistical results of the experimentation will be shown in Section V.

2) Face Detection Modality: A standard light weight fixed focus video camera can also be used to obtain the head movements by detecting the face movements of the user. The first step in video data analysis is to perform a histogram equalization of the RGB video data, aiming at improving contrasts and overcoming lighting variations. The resulted data is transformed to *YCbCr* space, to detect the skin color. The image is segmented to identify the skin, using threshold values for *Cb* and *Cr* previously obtained from training trials. An elliptical region of interest (ROI) is generated and centered at the first image moment of the segmented image. An operation *AND* is executed between the ellipsis generated and the negative of the Y-component (see Fig. 10).

The next step is the identification of the centroids of the regions associated with both eyes and mouth. For that, data are filtered using a Kalman filter to improve the position estimate. Three noncollinear points in the camera coordinates define a triangle in the image plane, as shown in Fig. 10. Changes in space points, due to head and face movements, are projected onto the image plane, thus changing the points in the image.

From the point projections on the image, different angles of the head movements can be obtained: rotation around Z-axis, rotation around Y-axis and rotation around X-axis, given, respectively, by the following expression:

$$\gamma = \tan^{-1}\left(\frac{yr - yl}{xr - xl}\right)$$

$$\beta = 2\tan^{-1}\left(\frac{a_1 \pm \sqrt{a_1^2 - f^2\left(\frac{a_1^2}{a_0^2} - 1\right)}}{f\left(\frac{a_1}{a_0} + 1\right)}\right)$$

$$\alpha = 2\tan^{-1}\left(\frac{c_1 \pm \sqrt{c_1^2 - f\left(\frac{c_1^2}{c_0^2} - 1\right)}}{f\left(\frac{c_1}{c_0} + 1\right)}\right).$$

Fig. 11 shows the use of a video camera to capture images of the user face, making possible to command the wheelchair by head movements [17].

Despite the fact that a *Kinect* camera provided by *Microsoft* can be also used for head motion detection, both webcam and *Kinect* are sensitive to lightening conditions (thus restricting the user's motion). Additionally, some users with cerebral palsy and with no accurate motor control of the head will not be able to use a head motion detection modality. Sip-and-puff or

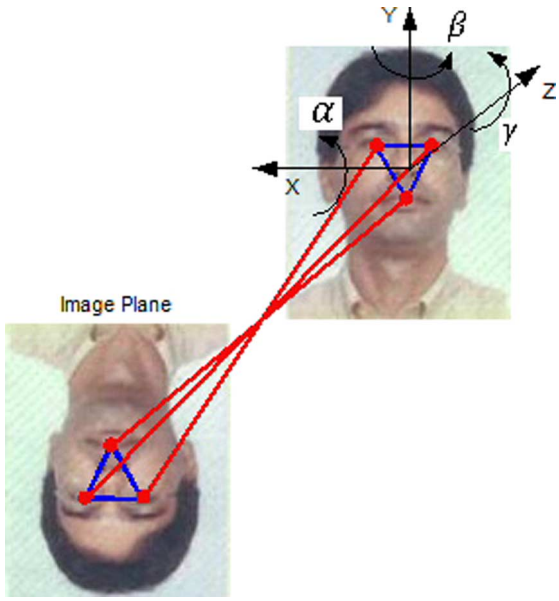

Fig. 10. Facial features.

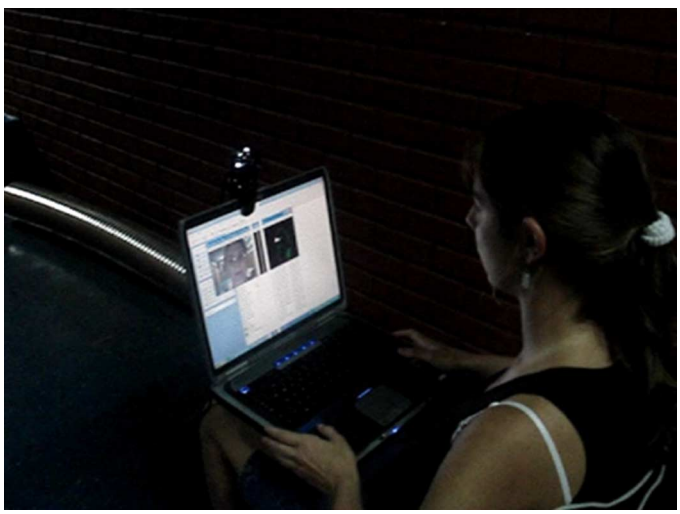

Fig. 11. Robotic wheelchair commanded by face movements (captured by a video camera).

eye movements can be preferred, which are other modalities of commanding the wheelchair presented in the following sections.

D. Robotic Wheelchair Commanded by Sip-and-Puff

Sip-and-puff can be used to command the wheelchair for users with ability to blow. In this modality, a pressure sensor, installed into a straw, allows users either choosing icons of movement (at the PDA's screen) to be executed by the wheelchair, or choosing destination places he/she wishes the wheelchair to go [18]. Fig. 12 shows a picture of a user commanding the wheelchair by sip-and-puff.

E. Robotic Wheelchair Commanded by Eye Movements

A webcam attached to a pair of glasses is used to command the wheelchair through detecting eye movements. The ocular globe is identified to obtain the eye movement information. This process requires a threshold identification to distinguish the iris

Fig. 12. User blows a straw to choose different options of movement or destination places to be executed or reached by the wheelchair.

Fig. 13. Robotic wheelchair commanded by eye movements.

from other parts of the face. However, this technique can be influenced by the presence of eyebrow and eyelash, which are eliminated by applying a Hough circular random transform and a Canny filter to the image [14], [19]. The next step is to define a ROI around the eye to allow tracking the eye movements. Due to illumination variations, a Kalman filter is used to reduce the error in the calculus of the eye center. Thus, the eyeball position is detected and tracked. The wheelchair user must gaze the eye to the symbol desired on the PDA screen in order to select it. For instance, to move the robotic wheelchair forward, the user must gaze his eye to the arrow representing the forward movement. Thus, the PDA will send a control signal to the computer onboard the wheelchair in order to start the desired movement (as shown in Fig. 4). Fig. 13 shows a picture of the HMI based on eye movements.

Compared to the interface based on eye blinks, the interface based on eye tracking provides a faster way of selecting symbols on the PDA and is more easily adapted to the user (it is just necessary a camera attached to a pair of glasses, as can be seen in Fig. 13). However, this interface is much more sensitive to noise (such as lighting changing and even eye blinks, as aforementioned). In both cases, the user needs to calibrate the system before using it. It is worth mentioning that the interface based on eye tracking is a simple and inexpensive alternative compared with commercial systems available in the literature [20].

By using the Canny filter combined with the random circular Hough transform, it is possible to accurately detect the iris of the eyeball and thus determine a region of interest, decreasing the influence of eyebrows and eyelashes in the calculation of the centroid of the iris. The use of the Kalman filter also enables fine-tuning of the eye-tracking movement.

However, there are people who cannot move the eyes, such as people in final stage of ALS, a situation named *locked-in*. For people with such kind of disability, another modality of wheelchair command is discussed in next section, which considers that most people suffering from ALS preserve their intellectual functions.

F. Robotic Wheelchair Commanded by Brain Waves

A BCI can use several paradigms to command a wheelchair, such as evoked potential P300 [21], motor imagery [22], or mental tasks [23]. Another paradigm is the steady state visual evoked potential (SSVEP). This potential is related to a visual flickering stimulation, and the frequency of this flickering stimulus will be present in the electroencephalogram (EEG) signal [24]. Hence, stimuli flickering at distinct frequencies can work simultaneously and be associated to different classes to be identified by a BCI [25].

In contrast with other BCIs, an SSVEP-BCI requires little user training and achieves high information transfer rate (ITR) [26]. Also, this kind of BCI is less susceptible to artifacts produced by eye blinks and eye movements, because the EEG signal, generally recorded in the occipital area, is far from the source of such artifacts [24].

Some researchers have used SSVEP-BCIs in wheelchair navigation tasks, such as the works developed in [27] and [28]. In [27], the interpretation of control commands generated by a SSVEP-BCI and how to use these commands in a finite state machine to navigate a simulated wheelchair are described. Three expert nonimpaired subjects participated in that study. The navigation task performed with this simulated wheelchair is to move it by a corridor. However, this work did not use a real wheelchair and executed only a simple navigation task. On the other hand, the work developed in [28] presents an equipped wheelchair to be operated from a SSVEP-BCI response. However, the wheelchair does not present a structure that allows it to be used by people with disabilities, once the stimulation and the processing units are located on the subject legs. Although this wheelchair has an autonomous navigation system, the eight healthy participants had to spend 10 min in training for BCI usage, in addition to be submitted to a previous calibration step.

The SSVEP-BCI here developed can work onboard a wheelchair, its structure is suitable for people with disabilities and its interface is easy to operate and configure. Moreover, calibration and training steps are not necessary.

Twelve EEG electrodes are used, which are placed over the occipital cortex (visual region), position P7, PO7, PO5, PO3, POz, PO4, PO6, PO8, P8, O1, O2, and Oz, according to Extend Standard International 10–20.

The users are then submitted to a visual stimulus, generated by a FPGA subsystem, composed by four black/white checkerboards stripes flickering at 5.6 rps (top), 6.4 rps (right), 6.9 rps (bottom), and 8.0 rps (left), as illustrated in Fig. 14. A yellow bar is used as biofeedback information to the user. The checkerboards flickering are measured according to their reversal patterns per second (rps).

Fig. 14. Robotic wheelchair commanded by the SSVEP-BCI developed.

EEG waves are temporally and spatially filtered and then features are extracted by a statistical test called spectral F-test (SFT). This test allows to detect phase-locked changes in the EEG signal recorded during the stimulation, $x[k]$, at a given stimulus frequency, $f0$, and thus to detect the evoked peaks related to this stimulus. SFT is applied as the ratio between the power in such frequency and the average power in L even neighboring frequencies [29]

$$\hat{\phi}_x(f_0) = \frac{P_{xx}(f_0)}{\frac{1}{L}\sum\limits_{\substack{i=-L/2 \\ i\neq 0}}^{i=L/2} P_{xx}(f_i)}$$

where $Pxx(f_0)$ is the power spectral density (PSD) of the signal $x[k]$ evaluated at the frequency f_0, and $Pxx(f_i)$ are the PSD values at the L neighbor frequencies closer to f_0. This statistical test is used to detect the evoked peaks rejected by the null hypothesis H_0 (absence of evoked response). This null hypothesis leads the power ratio presented above to be distributed according to an F distribution. Then a critical value is obtained for a significance level α, which is

$$SFT_{crit} = F_{2,2L,\alpha}.$$

This critical value corresponds to the rejection threshold of the null hypothesis H_0, and the evoked response will be considered for the values in the spectrum that are above of this critical value.

The features extracted are classified according to a decision tree developed for this application. Three attributes, A1, A2, and A3, were created and a decision tree responsible for classifying four classes is presented in Fig. 15.

The four classes are used to navigate the robotic wheelchair, moving it forward (top stripe), to the right (right stripe), to the left (left stripe), and stopping it (bottom stripe). Moreover, the stripes can be used to indicate or choose a final destination to the wheelchair (Fig. 16).

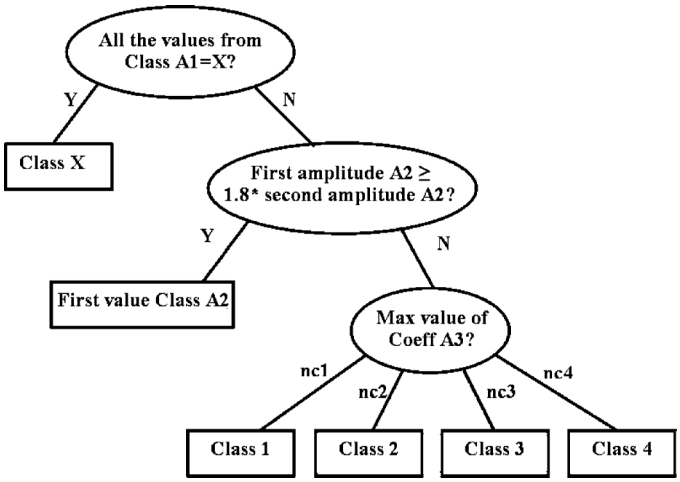

Fig. 15. Decision tree developed for the SSVEP-BCI.

Fig. 16. Visual stimuli used to choose the final destination.

G. Autonomous Navigation

The robotic wheelchair also provides an auto-guided option to the user for indoor environment navigation. This mode might be appropriate for highly dependent users, or a user who may desire this option to go to some specific locations in short time. Clearly, the autonomous navigation mode is aimed at reducing the user's effort in the generation of motion commands. It is worth mentioning that the autonomous navigation mode provided by the system (see Fig. 4) allows for the autonomous motion of the robotic wheelchair. However, the previously mentioned interface modalities allow for both the command of the wheelchair and the command of the PDA.

Two approaches of autonomous navigation have been developed in this work. The first approach consists of metallic tapes previously and strategically located at the environment's floor. Magnetic sensors are installed on the wheelchair, which detect the metallic tracks. The second approach is an SLAM-based path planning and navigation. This approach uses the range laser sensor mounted in the footrest of the wheelchair (see Fig. 2) to acquire information from the environment and to generate a consistent map of it. Such a map is then used to plan and follow different paths to destinations previously chosen by the user through the PDA.

One of the main differences among the two approaches is that the metallic tapes-based navigation is restricted by the disposition of such tapes. If a new environment needs to be accessible for the wheelchair's user, then new tapes must be placed there. However, the SLAM based navigation can be used despite the environment with no additional costs. One SLAM algorithm can be applied to all the environments with similar characteristics. In this work, we use a SLAM algorithm designed to manage lines—associated with walls—and corners extracted from the environment by means of the range laser sensor.

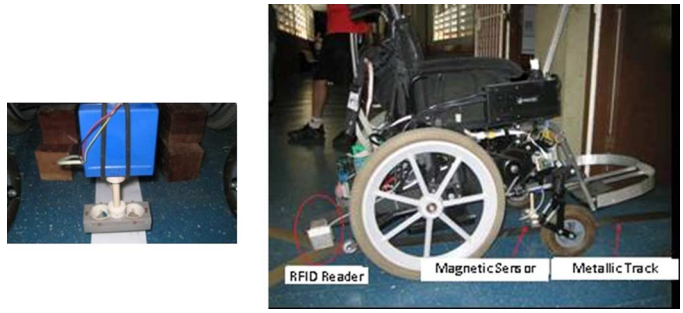

Fig. 17. Details of the magnetic sensor and its location on the wheelchair (left), and the RFID reader and the metallic tracks (right).

Following, each autonomous navigation approach will be explained in detail.

1) Metallic Tapes-Based Navigation: For this option, metallic tapes on the floor are provided to define the navigation path. Magnetic sensors are installed on the wheelchair, which detect the metallic tracks. In the auto-guided option, the pathway for the wheelchair along the metallic tapes, from the current location to the desired destination, is determined by the computer. RFID tags are also installed in suitable locations, such as doors, to calibrate the odometry. It also provides acoustic feedback to the user for location awareness. Fig. 17 shows the magnetic sensors and the RFID reader installed onboard the wheelchair.

The pros and cons of this mode of navigation are listed in Table I. Additionally, Fig. 18 shows an example of metallic tapes disposition within an apartment. As seen, the number of destinations is limited by the number of labels used to identify each room. It is worth mentioning that the PDA, in the autonomous modality interface, offers the user the different possible destinations when navigating through metallic tapes. Further information regarding how the user is able to manage and choose a destination through the PDA can be found in [30]. Briefly, the PDA displays all the available labels (related to the environment intended to navigate), and the user chooses one label as a destination (e.g., *kitchen*). Then, the wheelchair follows the metallic tapes by using its magnetic sensors as shown in Fig. 17. The position estimation is mainly based on odometric measurements, but RFID sensors are the ones that communicate the wheelchair that the user has reached the destination goal.

It is worth mentioning that the low level controller that relates the magnetic sensor readings with the motion commands is a PID controller. Additionally, we have set the maximum linear speed of the robotic wheelchair to 0.5 m/s, whereas the maximum rotational speed was set to 0.4 rad/s.

2) Slam-Based Navigation: Although metallic tapes are used along the path and magnetic sensors are used to detect them in order to allow the wheelchair to navigate through fixed ways,

TABLE I
PROS AND CONS OF METALLIC TAPES-BASED NAVIGATION

Pros	Cons
The disposition of the metallic tapes in the floor can be made in a way that dangerous or risky places can be avoided.	Environment conditioning and extra assistance are needed for disposition of metallic tapes and tags.
The disposition of the metallic tapes is related to the centrifugal force that the wheelchair could experiment when turning. Thus, we can minimize such force.	The user of the wheelchair only navigates following the metallic tapes. If the objective of the navigation remains out of the navigable path, then the user might not reach his/her desired destination nor perform the desired task.
The presence of metallic tapes indicates people the places where they should not be standing, in order to avoid obstacles during navigation.	The user is restricted to the places where the metallic tapes are located, thus restricting his/her independence. The latter might have a negative impact in user's perception and comfortability with the navigation system.
The metallic tapes disposition are useful for delicate maneuvering situations, such as crossing a door, motion through a narrow corridor, etc.	The localization of the wheelchair within the environment is made by dead-reckoning –whose errors are incrementally computed– and RFID readers, which increments the costs of installing this navigation modality.

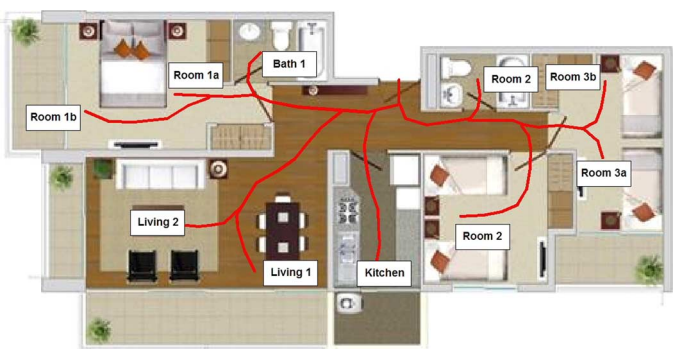

Fig. 18. Example of metallic tapes disposition (in solid red) within an apartment model.

such navigation strategy is highly restricted by the metallic tapes disposition, as shown in Table I. In order to fulfil the drawbacks shown by the previous navigation strategy, a SLAM algorithm is implemented in the robotic wheelchair system [31]. The SLAM algorithm uses the range readings—from the laser sensor mounted in the footrest of the wheelchair, as shown in Fig. 2—to concurrently localize the wheelchair within the environment and to build a geometric model—map—of such an environment. The latter is achieved by the implementation of an EKF (Extended Kalman Filter) based SLAM, that extracts corners—concave and convex—and lines—associated with walls—from the environment. The programming and optimization issues, and consistency results of the implemented EKF-SLAM can be found in a previous work of the authors [15], [32]. It is worth mentioning that the SLAM algorithm *per se*, is not a navigation strategy. It is an approach that can be

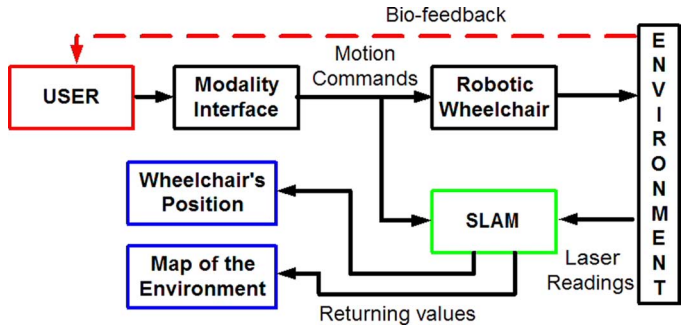

Fig. 19. Scheme of the SLAM algorithm as a secondary process during navigation.

used by a navigation strategy to enhance its performance. In this work, we have used the SLAM algorithm in the following situations:

1) to obtain an accurate map of an environment;
2) to allow for the performing of risky maneuvers.

To Obtain an Accurate Map: Considering that the aim of the SLAM algorithm is to build a map of the surrounding environment, such an algorithm performs as a secondary process whereas a user modality interface governs the wheelchair's motion, as shown in Fig. 19. An implemented example of this situation can be found in [15].

In Fig. 19, the user commands the wheelchair's motion through one of the modalities previously presented. The control commands as well as the laser sensor readings from the environment are the inputs of the EKF-SLAM algorithm [32]. The SLAM algorithm returns the instantaneous position of the wheelchair within the environment and a map of such environment. Thus, the SLAM algorithm is used only to model the environment that surrounds the wheelchair's navigation and to estimate the wheelchair's position. It is worth mentioning that the map of the environment and the position of the wheelchair within that environment, are obtained from the SLAM system state [32]. Furthermore, the SLAM algorithm is activated once the user selects the semi-autonomous navigation option shown in Fig. 4.

Additionally, the map of the environment can be stored within the wheelchair's onboard computer for future navigation purposes [30]. Fig. 20 shows an example of a map obtained from the EKF-SLAM algorithm used in this work. The magenta points are raw laser data, the solid dark segments are associated with extracted lines from the environment, whereas the green circles are the detected corners. The dotted blue line is the path traveled by the robotic wheelchair [13].

To Allow for the Performing of Risky Maneuvers: Based on the SLAM system state, we have available information regarding the environment surrounding the robotic wheelchair. Such information is used for two specific cases: crossing a door and turning within passageways. Both situations, although trivial, are of great efforts for the wheelchair's user. The crossing-a-door problem requires of precision, whereas the turning process requires precision and information regarding backward movements. The SLAM algorithm, in this case,

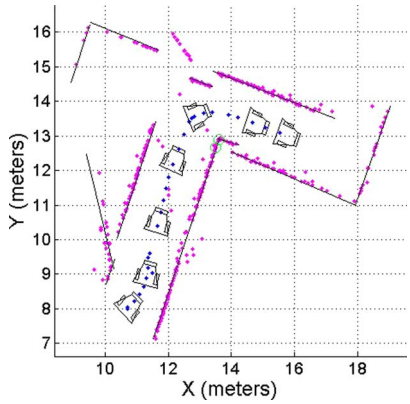

Fig. 20. Example of map obtained by the EKF-SLAM implemented in this work.

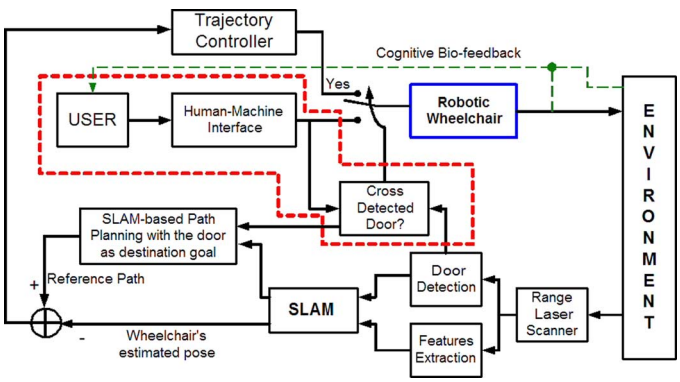

Fig. 21. General architecture of the SLAM-based crossing-a-door solution.

provides the necessary information to perform both process properly.

The crossing-a-door problem is summarized in Fig. 21.

The system architecture shown in Fig. 21 can be briefly summarized as follows.

- Within the dashed red line are the user-modality stages of the proposed architecture. The HMI (as the ones shown in this section) receives the user's physiological signals and generates motion commands with them, which are then imparted to the motorized wheelchair. In addition, the interface communicates to the user when a door has been detected. If more than one door was detected, the interface allows the user to choose which door to cross. The latter is accomplished by means of the same signals used to command the wheelchair's motion (see [33] for further details). If no door is chosen to cross, then the wheelchair motion control remains under the user decision. It is worth mentioning that the user's control stage is closed by a cognitive bio-feedback loop based on both the environment information and the perception of the wheelchair motion according to the user (dashed green line) [15].
- The range laser sensor mounted on the wheelchair's footrest shown in Fig. 2, is used to acquire the information regarding the surrounding environment. The raw range data acquired by the sensor is processed for doors detection and environmental features extraction. In particular, the door detection procedure is based on the histogram method [33] which obtains the Cartesian position of a door with respect to a reference frame attached to the vehicle. The features extracted from the environment correspond to lines—associated with walls—and corners—convex and concave. The detected doors and the features acquired from the environment are used by the SLAM algorithm. It is worth mentioning that the position of the detected doors is also part of the SLAM system state and it is used for localization purposes of the wheelchair.
- The map estimated by the SLAM algorithm is used for planning purposes. The Frontier Points Method [33] is used to locally plan a feasible and safe path between the wheelchair's position and the middle point of the door chosen by the user. The Frontier Points Method guarantees that a free collision path can be found within the mapped environment. Such a path is update at each sampling time of the SLAM algorithm. The reference path generated by the path planning stage is compared to the vehicle estimated position and such a comparison is fed to the trajectory controller. The trajectory controller used in our work is an adaptive trajectory controller with exponential stability [33].

If the user chooses to cross a detected door, then the control of the wheelchair switches to the trajectory controller. Hence, the crossing-a-door problem is performed autonomously. It is worth mentioning that the SLAM algorithm starts once the user chooses a detected door from the environment. After crossing the detected door, the SLAM memory usage is released from the onboard computer. More information regarding this implementation can be found in a previous work of the authors [33].

The second SLAM-based maneuver is a turning strategy that allows the user of the wheelchair to autonomously reach a desired orientation within a narrowed environment. This approach is useful for patients that present muscle spasms or loss of muscle activity, due to the great effort they have to make in order to perform backward movements. Briefly, the turning strategy uses the SLAM-based map for planning a suitable and safe collision path to be followed, autonomously, by the robotic wheelchair. Details of this implementation can be found in [13]. The method can be summarized as follows.

1) A visual interface allows the user to choose the desired orientation.
2) The computational system uses the map built by the SLAM algorithm and the estimate of the wheelchair position within the environment to check if there is enough space available for a safe navigation.
3) Following, a Monte Carlo based semi-circle generation searches for the minimum cost path based on successive generation of semi-circles of variable radius, as shown in Fig. 22 [13].
4) Once a path is found, a trajectory controller drives the wheelchair until it reaches a neighborhood of the desired orientation.

The proposed turning strategy guarantees the existence of a solution. Further details of this method can be found in [13]. Additionally, Fig. 22 shows an example of the turning strategy.

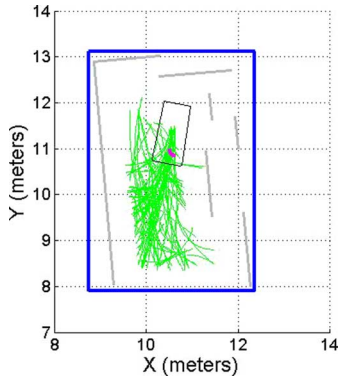

Fig. 22. Example of the turning strategy.

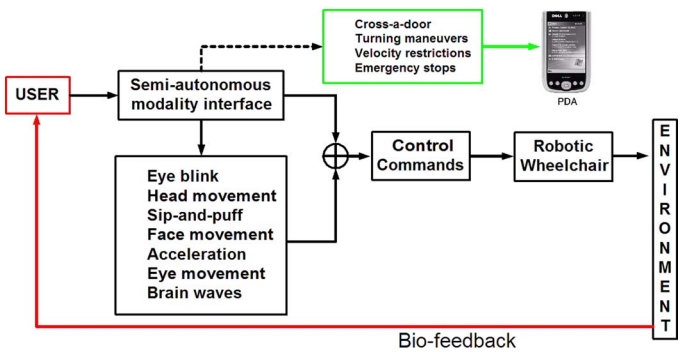

Fig. 23. Architecture of the semi-autonomous navigation.

In Fig. 22, the desired orientation is 180° from the current wheelchair's orientation—useful for passageways navigation–; the initial orientation of the wheelchair is $\theta = 1.4$ rads. The solid dark square represents the wheelchair within the environment; the solid green lines represent the successively feasible paths found by the system, whereas the solid magenta path is the one chosen as the optimum (according to a cost criterion presented in [13]). The solid grey segments are associated with lines extracted from the environment, whereas the solid blue rectangle circumscribes the map in order to restrict the maneuverability area. As can be seen, all feasible paths ensure a safe turning.

Once a path is chosen, the same trajectory controller presented in [33] is implemented to drive the wheelchair's motion until reaching the desired orientation.

H. Semi-Autonomous Navigation

Despite the user-dependent modalities shown in Fig. 4, the system can take the advantages of the autonomous implementation shown in Section III-G2 to assist the user on the wheelchair ([34]). With this insight, a semi-autonomous modality is proposed.

This modality assists the user in a secondary way (as shown in Fig. 23) and it is explained as follows.

- Once the user chooses to control the robotic wheelchair in a semi-autonomous way, the only changes experienced by the user is in the control of the device. Thus, the interface remains the same. In fact, it could be one of the seven modalities presented in this work (shown in Fig. 4): eye blink, eye movement, face movement, head movement, acceleration, sip-and-puff and brain waves.
- The control of the wheelchair is based on a fusion of the user's command generation through her/his modality and four autonomous executions: *crossing-a-door*, *turning maneuvers*, *emergency stops*, and *velocity restrictions*, which are automatically executed once the user chooses the semi-autonomous navigation modality.
- Such four automatic executions are aimed at protecting and assisting the user in the following manner.
  1) *Crossing-a-door*: the strategy presented in Section III-G2 for detecting and crossing doors is executed. It is always processing range data (acquired from the laser implemented at the wheelchair's footrest, as shown in Fig. 2) in order to detect possible doors. Once a door (or more) is detected, it shows to the user the detected doors through the PDA. If the user chooses to cross such a door, then the SLAM algorithm is used to fulfil the task, as previously stated. The user is also able to ignore the detected doors and continue the navigation (in [33], further details are provided regarding the crossing-a-door system).
  2) *Turning maneuvers*: if the system detects that the wheelchair is maneuvering within confined spaces, the option of turning is automatically visible in the PDA. The details regarding how the system detects the restrictions in the workspace can be found in a previous work of the authors [13].
  3) *Emergency stops*: the laser mounted at the wheelchair's footrest is always acquiring readings from the environment. If the wheelchair is too close to a detected obstacle (e.g., a person blocking the passageway) the wheelchair stops its navigation and blocks further movements in the direction of collision. Thus, the *emergency stop* stage prevents the user of collisions. It is worth mentioning that the *emergency stop* is not an option of the system, it is always performing despite the interface modality. However, during the *crossing-a-door* or *turning maneuvers* executions, the *emergency stop* is not attended due to the fact that both executions already have an emergency stop strategy per se (see [15] and [33]).
  4) *Velocity restrictions*: in the first two cases (*crossing-a-door* and *turning maneuvers*) the velocity of the vehicle was generated according to the trajectory follower controller implemented in [13], [33] respectively. However, when the robotic wheelchair is commanded directly by the user, considerations regarding the maximum permissible speeds must be taken into account, in order to protect the user and wheelchair's integrity. Thus, when selected the semi-autonomous modality, the maximum linear speed of the wheelchair is set to $v_{\max} = 0.5$ m/s, whereas the angular velocity is set to $w_t = w_{\max} * \cos(\alpha * v_t)$ rad/s, where v_t is the instantaneous linear velocity and $w_{\max} = \pi/3$ rad/s, the maximum angular velocity. The expression used to determine the angular velocity is intended to regulate

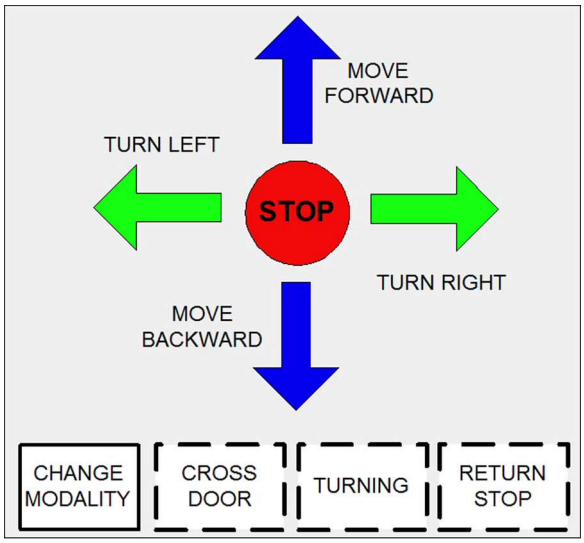

(a)

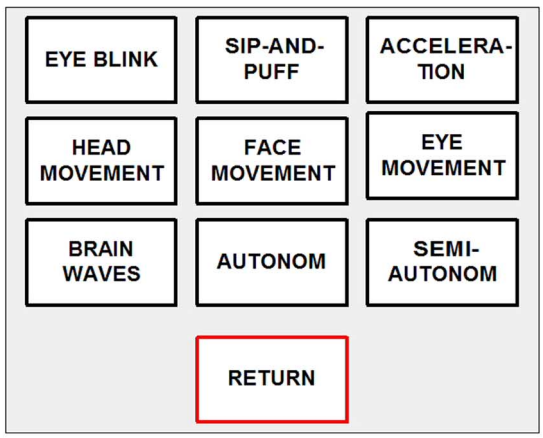

(b)

Fig. 24. Visual interfaces for commanding the robotic wheelchair motion.

the turning. Thus, the higher the linear velocity, the smaller the angular velocity. Hence, the centrifuge force can be controlled. Additionally, $0 < \alpha \leq 1$ is a design parameter.

IV. Navigation Interface

Despite the modality chosen by the user, the volunteer must be able to command the wheelchair's motion and to choose the modality *per se*. Fig. 24 shows the visual and basic interface implemented in this work for commanding the multi-modality system. The way the system recognizes a valid command using the different modalities, can be seen in the previous works of the authors [14]–[16], [18], [30], [33]. Briefly,

1) By a sequential scanning method [30], the volunteers can choose one of the following motion commands from the visual interface shown in Fig. 24(a): *move forward*, *move backward*, *turn to the left*, *turn to the right*, and *stop motion*. However, she/he can also choose one of the following combination of movements: *move forward while turning to the left*, *move forward while turning to the right*, *move backward while turning to the left*, *move backward while turning to the right*. It is worth mentioning that, in the last four cases, the velocity restrictions of the robotic wheelchair presented in Section III-F are applied. Additionally, the volunteer can choose among remaining in the same modality or changing it.
2) If the *semi-autonomous* modality was on, then the dashed blocks *cross a door*, *turning*, and *returning from stop* would have been available for the user.
3) If the volunteers choose to change the current modality, then the visual interface shown in Fig. 24(b) is shown to the user through the PDA. As in the previous interface, the one shown in Fig. 24(b) is also sequentially scanned among all the possible modalities presented in this work (see Fig. 4). If a different modality is chosen, the system automatically starts to be governed by such modality. If the volunteer chooses to *return*, then the interface shown in Fig. 24(a) is displayed through the PDA.
4) If the volunteer chooses the *semi-autonomous* modality, then other *nonautonomous* modality must be also chosen, as stated in Section III-H. In this case *cross a door*, *turning* and *returning from stop* are available to the user.
5) *Cross a door* is highlighted once a door—or several doors—is detected [33]. The reenlightening disappears once the user chooses to ignore the crossing-a-door problem [33].
6) *Turning* is highlighted once the system detects that the wheelchair is navigating through confined spaces. Additionally, it can be activated at will by the user as shown in [13].
7) *Returning from stop* is highlighted when an emergency stop generated by the *semi-autonomous* modality takes place. The user can deactivate such emergency stop by accessing the highlighted block.

In the following section, the experimental results of the proposed multi-modality system are presented.

V. Experimental Results and Discussions

The wheelchair using the modality-independent HMI so far described was guided by a set of healthy and disabled volunteers. All the experimental protocols were approved by the Ethic Committee of the Federal University of Espirito Santo, UFES, Brazil, the research institution responsible for this project, and have been executed after getting the signatures of the volunteers in a consent form previously presented to them.

This section presents the volunteers, the questionnaire used by them to evaluate each modality interface, the associated statistical results and metric results obtained during the experimentation. The evaluation and experimentation of each modality shown in Fig. 4 is presented herein.

A. Questionnaire and Population

A population of seven patients with different disabilities tested the multi-modality system presented in this work. However, depending on the nature of the interface, some volunteers were not able to command a specific kind of modality. Thus, four patients presented lower limb paralysis (two males of 28 and 34 years old, respectively, and two females of 24 and 30 years old volunteers V1–V4), one patient presented Duchenne dystrophy (male, of 15 years old volunteer V5), and two male

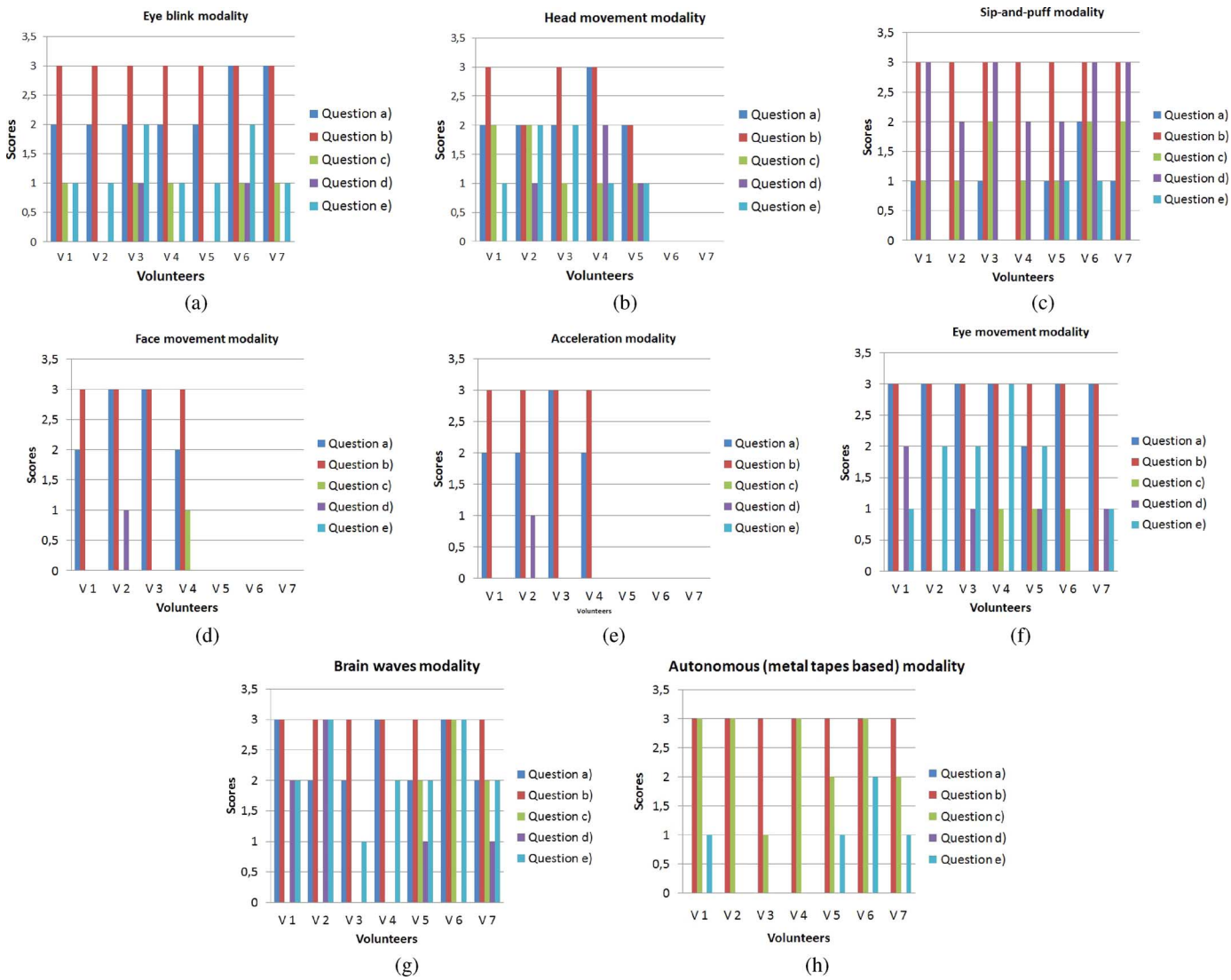

Fig. 25. Statistical results for each modality.

volunteers of 29 and 31 years old, with paraplegia level T9-T10 and paralysis level T1, respectively, volunteers V6-V7. All volunteers signed a consent form before the trials.

After the experimentation, each volunteer filled out a questionnaire, with five questions regarding the modality performance and the user comfort, shown as follows.

1) Which was your difficulty level in commanding the wheelchair with this modality?
2) Do you think that you achieved the destination goal? (score 3 for yes, 0 for no).
3) Do you think that this modality has improved your mobility? (score between 3—for high improvement–to 0—nonacceptable improvement).
4) Do feel tired after the trials? (score between 3—for very tired—to 0—no tired).
5) Did you feel comfortable using this modality? (score between 3—for very comfortable—to 0—no comfortable at all).

The trial consisted of a point-to-point navigation. The robotic wheelchair started from an initial position and had to reach a desired destination within another room of the environment. In order to do so, the modalities presented in Fig. 4 were tested for each one of the volunteers mentioned before. The answers to the questionnaire were the following [35]: *Without any difficulty = 3*, *With some difficulty = 2*, *With much difficulty = 1*, *Unable to do = 0*. Fig. 25 shows the statistic results corresponding to each modality and each volunteer. The questionnaire was filled out once the volunteers finished ten trials for each modality. Additionally, not all the volunteers were able to perform all the available modalities. Such a discussion is included in the sequel.

Several conclusions can be obtained by inspection of Fig. 25. Thus,

1) *Eye blink modality*. The users agreed that this modality is ease to command and that they all achieved the destination goal. However, the first four volunteers (the patients with lower limb paralysis) do not consider that the modality actually improved their mobility (when compared with a manual drive of the wheelchair). Nevertheless, the remaining three volunteers do agree that the modality had improved their mobility. Additionally, the seven volun-

teers agreed that they felt tired after the trials and that the modality is not very comfortable.

2) *Head movement modality*. In this modality, V6 and V7 did not performed the trials. The five volunteers agreed that they have reached the destination point. Specially the four first volunteers found the modality ease to command. In average, the volunteers did not find that this modality had improved their mobility, mainly due to the fact that the four first volunteers (V1–V4) were able to drive manually the wheelchair. It is important to note that V5 experienced tiredness after the trial.
3) *Sip-and-puff modality*. As in the previous modalities, all volunteers considered that they reached the destination goal. Unlike the previous modality, the sip-and-puff approach was able to be commanded by the seven volunteers. Volunteers V1–V4 considered that the modality did not improve their mobility (when compared to manually drive of the wheelchair). However, V5–V7 showed an important improvement compared to the previous modalities. However, all volunteers agreed regarding the tiredness they felt after the trials.
4) *Face movement and Acceleration modality*. Due to their capabilities, only V1–V4 were able to command the wheelchair under this modality. As in *head movement* modality, the users did not find an important improvement in their modality and all found that they reached the destination goal. Additionally, they expressed their lack of comfortability in using this modality.
5) *Eye movement modality*. As *sip-and-puff*, this modality was commanded by all the volunteers. V1–V7 found that this modality did not add any improvement to their mobility. However, all volunteers expressed that they did not find any difficulty in commanding the wheelchair. As in the previous cases, all the volunteers considered that they reached the destination goal.
6) *Brain waves modality*. As in the previous cases, the volunteers answered that they reached the destination goal. However, it is worth mentioning that this modality has highly improved the mobility of V5–V7 with respect to the other modalities.
7) *Autonomous navigation*. In this modality, all volunteers agreed that the modality had improved their mobility. However, it is interesting to note that all the volunteers had expressed their lack of comfortability in using the autonomous navigation approach, mainly due to their possible lack of confidence on unmanned vehicles.

As can be seen, the presented system offers the user a wide range of modality, that she/he can select according to her/his capabilities.

Additionally, Fig. 26 shows the different paths traveled by the robotic wheelchair for each experimentation. Each trial was repeated ten times from different initial positions to different final destinations and for each modality. Although, for visualization purposes, Fig. 26 shows only two cases for each volunteer (using the *sip-and-puff* modality). The trials of the entire system were performed during one year. Each modality was tested during one month by the volunteers, thus avoiding excessive effort. The initial position of the wheelchair is marked with a solid red dot, whereas the final destination is marked with solid green dots; magenta points represent raw laser data—acquired from the laser range sensor mounted at the wheelchair's footrest, see Fig. 2. The paths traveled by the wheelchair are drawn in solid blue and solid black lines for the two trials shown herein.

In Fig. 26 it is interesting to note that, despite the users' answers in Fig. 25, they did not reached the destination goal. Instead, they considered the destination goal as reached once they entered to the room where such destination was located. The navigation results of the autonomous modality are not shown since the metal tapes drove the wheelchair's motion until reaching the desired destination goal precisely. Additionally, Fig. 26 shows the risky maneuvers performed by the users in order to cross doors.

Fig. 27 shows the mean (solid dark line) and standard deviation (in grey) of the distances between the destination goal and the location where the volunteers stopped the motion because they considered the destination as reached. Fig. 27 give us important information of how the volunteers perceive the navigation trial. This figure was obtained by using the estimation of the wheelchair's location within the environment. In order to do so, the SLAM algorithm was running during the trials. Additionally, Fig. 28 shows the mean and standard deviation of the time needed for each volunteer in fulfil the task according the *brain waves* modality. In magenta one can see the mean and standard deviation of the time associated with each volunteer without considering the *semi-autonomous* modality—mentioned in Section III-G2. However, we have repeated the same trials but with the *semi-autonomous* modality performing, i.e., the user was assisted during crossing-a-door situations and during turnings. In grey, Fig. 28 shows the mean and standard deviation associated with the *semi-autonomous* modality. As can be seen, the time required to achieve the task is reduced. However, the users experimented their lack of comfortability when operating autonomously, as previously stated.

It is interesting to note in Fig. 28 that volunteers V1–V4 had experienced a higher execution time than volunteers V5–V7. The use of the *semi-autonomous* modality has improved the usage time of the robotic wheelchair, but also the results shown in Fig. 28 depict the learning experienced by the volunteers while using the robotic device.

VI. Conclusion

A new modality-independent interface to command a robotic wheelchair was presented in this paper. Such wheelchair can be commanded by eye blinks, eye movements, head movements, sip-and-puff and brain waves. The wheelchair can also navigate in an autonomous mode, taking the user from the current location to a desired one, or following metallic tracks, in an auto-guided mode. RFID was used to calibrate the odometry and to provide location feedback to the user.

The wheelchair was provided with a user friendly GUI interface, which the user can use to navigate the wheelchair or communicate with people around. The GUI is composed of icons which can be arrows characterizing movements or destination places. In addition to these icons, there are other icons to help the user to express his/her emotions and feelings, or to select characters to compose words or sentences. A set of prerecorded

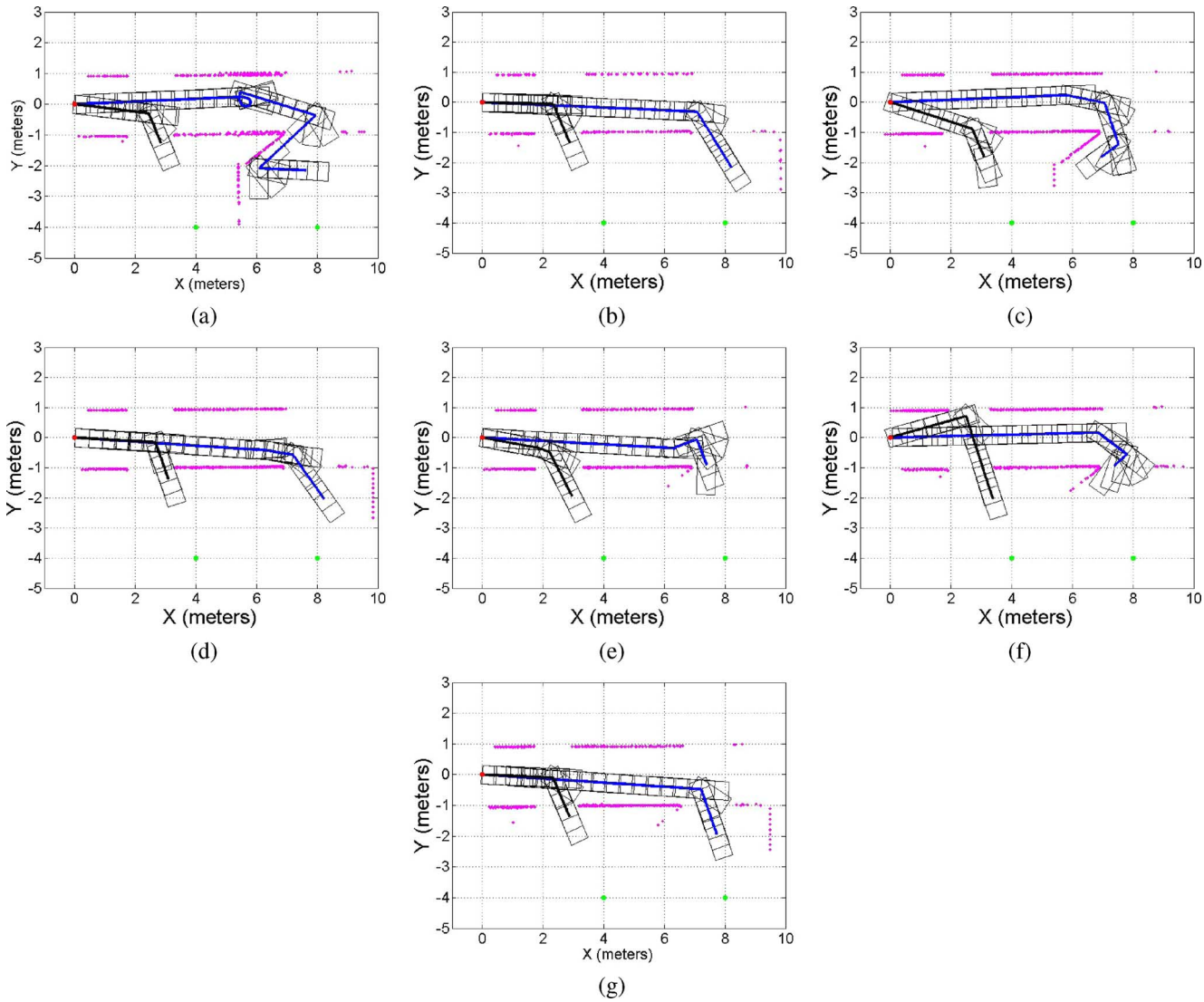

Fig. 26. Navigation results for two trials of the *sip-and-puff* modality. Fig. 26(a)–(g) correspond to the navigation results of V1–V7, respectively.

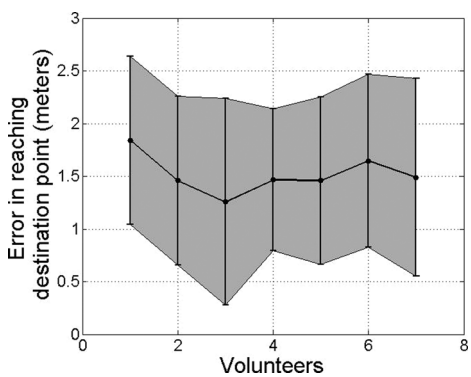

Fig. 27. Mean and standard deviation of the distances between the navigation goal and the position where the user considers that she/he has reached such a destination.

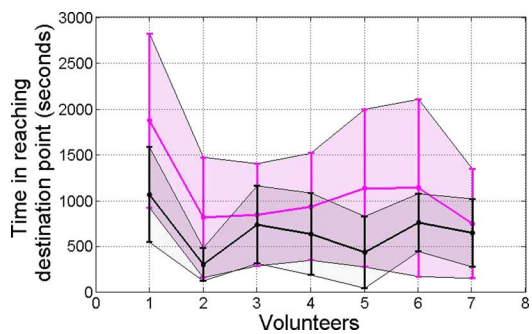

Fig. 28. Mean—solid line—and standard deviation of the time required for each user to complete the task with the *brain waves* modality according to both a *nonautonomous* and a *semi-autonomous* modality.

acoustic signals and a speaker onboard the wheelchair is provided for this purpose.

Kinematics and dynamic model-based control architectures were used to control the wheelchair movement. The kinematic controller manages the wheelchair's orientation and its linear and angular velocities, whereas the dynamic controller allows for generating smooth movements of the wheelchair. There is also a supervisor that can receive inputs from the user onboard the wheelchair, allowing the user to help the control system to manage obstacles in a more efficient way.

Several experiments were conducted with this robotic wheelchair, using different command modalities. The wheelchair was evaluated by healthy people and people with disabilities (adult and children), and got their approval, in addition to fill out a questionnaire, with five questions regarding the modality performance and the user comfort. The associated statistical results and metric results obtained during the experimentation were also shown.

The next step involves only the BCI here described: it will be extended to include the possibility of using motor imagery and signals from the Broca area of the brain. This option would allow the user to command intuitively the wheelchair with the intention of the movement of the left and right hand, and imagination of random words starting with the same letter. Preliminary experiments have been conducted using PSD and adaptive autoregressive parameters as feature inputs to a classifier based on support vector machine, and have shown encouraging possibilities.

REFERENCES

[1] C. R. Cassemiro and C. G. Arce, "Visual communication by computer in amyotrophic lateral sclerosis," *Arquivos Brasileiros de Oftalmologia*, vol. 67, no. 2, pp. 295–300, 2004.

[2] C. F. Borges, "Dependency and die of the family mother: The helping from family and community to take care of a pacient with amyotrophic lateral sclerosis," *Psicologia em Estudo*, vol. 8, pp. 21–29, 2003.

[3] R. Barea, L. Boquete, M. Mazo, and E. Lopez, "Wheelchair guidance strategies using EOG," *J. Intell. Robot. Syst.*, vol. 34, pp. 279–299, 2002.

[4] R. C. Simpson, "Smart wheelchairs: A literature review," *J. Rehabil. Res. Develop.*, vol. 42, pp. 423–436, 2005.

[5] K. Tanaka, K. Matsunaga, and H. Wang, "Electroencephalogram-based control of an electric wheelchair," *IEEE Trans. Robot.*, vol. 21, no. 4, pp. 762–766, 2005.

[6] S. Ronnback, On methods for assistive mobile robots Dept. Comput. Sci. Electr. Eng., Lulea Univ. Technol., 2006 [Online]. Available: http://epubl.ltu.se

[7] A. Teymourian, T. Luth, A. Graser, T. Felzer, and R. Nordmann, "Braincontrolled finite state machine for wheelchair navigation," in *Proc. 10th Int. ACM SIGACCESS Conf. Comput. Accessabil.*, 2008, pp. 257–258.

[8] C. Mandel, T. Luth, T. Laue, T. Rofer, A. Graser, and B. Krieg-Bruckner, "Navigating a smart wheelchair with a brain-computer interface interpreting steady-state visual evoked potentials," in *Proc. IEEE/RSJ Int. Conf. Intell. Robots Syst.*, 2009, pp. 1118–1125.

[9] H. Soh and Y. Demiris, "Involving young children in the development of a safe, smart paediatric wheelchair," presented at the ACM/IEEE HRI-2011 Pioneers Workshop, Lausanne, Switzerland, 2011.

[10] Y. Nam, Q. Zhao, and A. Cichocky, "Tongue-rudder: A glossokinetic-potential-based tongue-machine interface," *IEEE Trans. Biomed. Eng.*, vol. 59, no. 1, pp. 290–299, Jan. 2012.

[11] C. Gao, T. Miller, J. Spletzer, I. Hoffman, and T. Panzarella, "Autonomous docking of a smart wheelchair for the automated transport and retrieval system (ATRS)," *J. Field Robot.*, vol. 25, no. 4-5, pp. 203–222, 2008.

[12] A. Kubler, B. Kotchoubey, J. Kaiser, J. R. Wolpaw, and N. Birbaumer, "Braincomputer communication: Unlocking the locked in," *Psychol. Bull.*, vol. 127, no. 3, pp. 358–375, 2001.

[13] F. A. A. Cheein, C. D. la Cruz, T. F. Bastos-Filho, and R. Carelli, "Navegacion autonoma asistida basada en SLAM para una silla de ruedas robotizada en entornos restringidos," *Revista Iberoamericana de Autom. e Inform. Indust. RIAI*, vol. 8, no. 2, pp. 81–92, 2011.

[14] T. F. Bastos, M. Sarcinelli-Filho, A. Ferreira, W. C. Celeste, R. L. Silva, V. R. Martins, D. C. Cavalieri, P. S. Filgueira, and I. B. Arantes, "Case study: Cognitive control of a robotic wheelchair," in *Wearable Robots: Biomechatronic Exoskeletons*. New York: Wiley, 2008, ch. 9.

[15] F. A. A. Cheein, N. Lopez, C. Soria, F. L. Pereira, F. di Sciascio, and R. Carelli, "Slam algorithm applied to robotic assistance for navigation in unknown environments," *J. Neuroeng. Rehabil.*, vol. 7, no. 10, pp. 1–15, 2010.

[16] E. Perez, C. Soria, M. Bortole, T. F. Bastos-Filho, and V. Mut, "Fusion of head angles to command a robotic wheelchair," in *Proc. Biosign. Robot. Better Safer Living*, Vitoria, Brazil, 2010, pp. 1–6.

[17] C. D. la Cruz, T. F. Bastos-Filho, and R. Carelli, "Adaptive motion control law of a robotic wheelchair," *Control Eng. Practice*, vol. 19, pp. 113–125, 2011.

[18] P. F. S. Amaral, J. C. Garcia, T. F. Bastos-Filho, and M. Mazo, "Ambient assisted route planner based on xml files with accessibility information," in *Proc. 6th IEEE Int. Symp. Intell. Signal Process.*, 2009, pp. 147–152.

[19] S.-H. Chiu and J.-J. Liaw, "A proposed circle/circular arc detection method using the modified randomized Hough transform," *J. Chin. Inst. Eng.*, vol. 29, no. 3, pp. 533–538, 2006.

[20] E. Schneider, K. Bartl, S. Bardins, T. Dera, G. Boening, and T. Brandt, "Eye movement driven head-mounted camera: It looks where the eyes look," in *Proc. IEEE Int. Conf. Syst., Man Cybern.*, 2005, vol. 3, pp. 2437–2442.

[21] G. Pires, U. Nunes, and M. Castelo-Branco, "Statistical spatial filtering for a P300-based BCI: Tests in able-bodied, and patients with cerebral palsy and amyotrophic lateral sclerosis," *J. Neurosci. Methods*, vol. 195, pp. 270–281, 2011.

[22] F. Cincotti, D. Mattia, F. Aloise, S. Bufalari, L. Astolfi, F. D. V. Fallani, A. Tocci, L. Bianchi, M. G. Marciani, S. Gao, J. Millan, and F. Babiloni, "High-resolution EEG techniques for brain-computer interface applications," *J. Neursci. Methods*, vol. 167, pp. 31–42, 2008.

[23] F. Faradji, R. K. Ward, and G. E. Birch, "Plausibility assessment of a 2-state self-paced mental task-based BCI using the no-control performance analysis," *J. Neursci. Methods*, vol. 180, pp. 330–339, 2009.

[24] F.-B. Vialatte, M. Maurice, J. Dauwels, and A. Cichocki, "Steady-state visually evoked potentials: Focus on essential paradigms and future perspectives," *Prog. Neurobiol.*, vol. 90, pp. 418–438, 2010.

[25] C. Ming and G. Shangkai, "An EEG -based cursor control system," in *Proc. 1st Joint BMES/EMBS Conf.*, 1999, vol. 1, p. 699.

[26] B. Y. Wang, X. Gao, B. Hong, C. Jia, and S. Gao, "Brain computer interfaces based on visual evoked potentials—Feasibility of practical system designs," *IEEE Eng. Med. Biol. Mag.*, pp. 64–71, Sep./Oct. 2008.

[27] A. Teymourian, T. Lüth, A. Gräser, T. Felzer, and R. Nordmann, "Brain-controlled finite state machine for wheelchair navigation," in *Proc. 10th Int. ACM SIGACCESS Conf. Comput. Accessibil.*, 2008, pp. 257–258.

[28] C. Mandel, T. Luth, T. Laue, T. Rofer, A. Gräser, and B. Krieg-Brückner, "Navigating a smart wheelchair with a brain-computer interface interpreting steady-state visual evoked potentials," in *Proc. IEEE/RSJ Int. Conf. Intell. Robots Syst.*, 2009, pp. 1118–1125.

[29] A. M. F. L. M. de Sá, H. C. Thiengo, I. S. Antunes, and D. M. Simpson, "Assessing time- and phase-locked changes in the EEG during sensory stimulation by means of spectral techniques," in *Proc. IFMBE*, 2009, vol. 25, pp. 2136–2139.

[30] F. A. Cheein, R. Carelli, W. C. Celeste, T. F. Bastos, and F. di Sciascio, "Maps managing interface design for a mobile robot navigation," in *J. Phys. Conf. Ser.*, 2007, vol. 90, p. 012088.

[31] S. L. G. Ippoliti and L. Jetto, "Localization of mobile robots: Development and comparative evaluation of algorithms based on odometric and inertial sensors," *J. Field Robot.*, vol. 22, no. 12, pp. 725–735, 2005.

[32] F. A. A. Cheein and R. Carelli, "Analysis of different features selection criteria based on a covariance convergence perspective for a SLAM algorithm," *Sensors (Basel)*, vol. 11, no. 1, pp. 62–89, 2011.

[33] F. A. A. Cheein, C. De la Cruz, T. F. Bastos-Filho, and R. Carelli, "Slam-based cross-a-door solution approach for a robotic wheelchair," *Int. J. Adv. Robot. Syst.*, vol. 6, no. 3, pp. 239–248, 2009.

[34] E. C. D. Kulic, "Safe planning for human-robot interaction," *J. Field Robot.*, vol. 22, no. 7, pp. 383–396, 2005.

[35] F. Wolfe, "A brief clinical health assessment instrument: Clinhaq," *Arthritis Rheum.*, vol. 32, p. C49, 1989.

Teodiano Freire Bastos-Filho graduated in electrical engineering from the Universidade Federal do Espírito Santo, Vitória, Brazil, in 1987, and received the Ph.D. degree in physical sciences from the Universidad Complutense de Madrid, Madrid, Spain, in 1994.

He is with the Department of Electrical Engineering, Universidade Federal do Espírito Santo, Vitória, Brazil, and with the Brazilian National Council for Scientific and Technological Development (CNPq). His research interests are signal processing, rehabilitation robotics and assistive technologies.

Fernando Auat Cheein (M'12) received the B.Sc. degree in electronic engineering from the National University of Tucuman, Tucuman, Argentina, in 2002, and the Ph.D. degree in control systems engineering from the National University of San Juan, San Juan, Argentina, in 2009.

From 2009 to 2011, he was involved in Argentinean projects of robotics applied to agriculture. Currently, he is with the Department of Electronic Engineering, Universidad Tecnica Federico Santa Maria, Valparaiso, Chile, working in projects related to unmanned robots in olive groves. His research interests also include autonomous SLAM and path planning.

Sandra Mara Torres Müller received the B.Sc., M.Sc. and Ph.D. degrees in electrical engineering from the Federal University of Espírito Santo, Vitória, ES, Brazil, in 2003, 2006, and 2012, respectively.

She is currently with the Department of Computer and Electronics of the Federal University of Espírito Santo, São Mateus, ES, Brazil. Her research interests are in signal processing, biological signal processing, pattern recognition, and brain–computer interfaces.

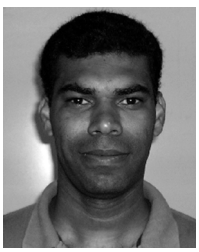

Wanderley Cardoso Celeste received the B.Sc., M.Sc., and Ph.D. degrees in electrical engineering from the Federal University of Espírito Santo, Vitória, ES, Brazil, in 2002, 2005, and 2009, respectively.

He is currently with the Department of Computer and Electronics of the Federal University of Espírito Santo, São Mateus, ES, Brazil, where he is a permanent member of the Graduate Program on Energy. His research interests are automation and control systems.

Celso de la Cruz received the B.Sc. degree in mechanical engineering from the Universidad Nacional del Centro, Huancayo, Peru, in 1996, the M.Sc. degree in control and automation engineering from the Pontificia Universidad Católica, Lima, Peru, 1999, and the Ph.D. degree in control systems engineering from the National University of San Juan, San Juan, Argentina, in 2006.

His research interests are mechatronics, with emphasis in control, and control of multi-robot formations.

Daniel Cruz Cavalieri received the B.Sc. degree in electrical engineering from the Federal University of Viçosa, Viçosa, MG, Brazil, in 2005, and the M.Sc. and Ph.D. degrees in electrical engineering from the Federal University of Espírito Santo, Vitória, ES, Brazil, in 2008 and 2013, respectively.

His research interests are natural language processing, human–machine interfaces, and assistive technologies.

Mário Sarcinelli-Filho received the B.Sc. degree from Federal University of Espírito Santo, Vitória, ES, Brazil, in 1979, and the M.Sc. and Ph.D. degrees from Federal University of Rio de Janeiro, Rio de Janeiro, Brazil, in 1983 and 1990, respectively, all in electrical engineering.

He is with the Department of Electrical Engineering, Federal University of Espírito Santo, and the Brazilian National Council for Scientific and Technological Development (CNPq). His research interests are signal and image processing, brain–computer interfaces, mobile robotics, coordinated control of mobile robots, and unmanned aerial vehicles.

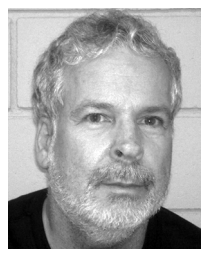

Paulo Faria Santos Amaral received the B.Sc. degree in electronic engineer from the Technological Institute of Aeronautics, São José dos Campos, SP, Brazil, in 1976, the M.Sc. degree in electronic engineering from the National Institute of Spacial Research, Brazil, São José dos Campos, SP, Brazil, in 1979, and the Ph.D. degree in electrical engineering from the University of São Paulo, São Paulo, SP, Brazil, in 1985.

He has retired from the Federal University of Espírito Santo, Brazil, where he was an Associate Professor at the Department of Electrical Engineering.

Elisa Perez graduated in biomedical engineering, in 2004, from the National University of San Juan, San Juan, Argentina, where she received the Ph.D. degree in control systems engineering, in 2010.

She is currently an Associate Professor at the National University of San Juan, San Juan, Argentina. Her research interests are image processing, human–computer interfaces, and control of robotic wheelchairs.

Carlos Miguel Soria graduated in electrical engineering from the National University of Tucuman, Tucuman, Argentina, in 1996, and the M.Sc. and Ph.D. degrees in control systems engineering from the National University of San Juan, San Juan, Argentina, in 2000 and 2005, respectively.

He is presently Associate Professor at the National University of San Juan and Assistant Researcher of the National Council for Scientific and Technical Research (CONICET, Argentina). His research interests are control of manipulators and mobile robots, computer vision, and sensorial integration.

Ricardo Carelli (M'76–SM'98) was born in San Juan, Argentina. He graduated in engineering from the National University of San Juan, San Juan, Argentina, and received the Ph.D. degree in electrical engineering from the National University of Mexico, Mexico City, Mexico.

He is full Professor at the National University of San Juan, where he is Director of the Instituto de Automática, and Senior Researcher of the National Council for Scientific and Technical Research (CONICET, Argentina). His research interests are on robotics, manufacturing systems, adaptive control and artificial intelligence applied to automatic control.